EFFECTIVE-FOURTH-ORDER RESONATOR BASED MASH BANDPASS SIGMA-DELTA MODULATORS

Mohammed Al-Janabi, Izzet Kale and Richard C.S. Morling

University of Westminster
School of Electronic and Manufacturing Systems Engineering
115 New Cavendish St., London WIM 8JS, UK
email: mohammed@cmsa.westminster.ac.uk

ABSTRACT

Two novel effective-fourth-order (eighth-order) resonator based MASH bandpass Σ–Δ modulators are introduced at the behavioural level and subsequently examined by simulations utilising the ALTA SPW environment. The considered bandpass configurations have in their loop filter a cascade of standard second-order resonator structures in order to achieve appropriate noise shaping. The quantisation noise in each stage is suppressed by feeding the error of each section into the input of the following stage. It is demonstrated in this paper that the quadruple effective-first-order cascade configuration has significantly better performance as well as conforming more closely with theory in comparison with the effective-second-order effective-second-order cascade. The superior performance of the former can be attributed to the cumulative effect of the multi-bit outputs as well as the presence of more notch filters.

1. INTRODUCTION

Concepts of standard oversampled sigma-delta (Σ–Δ) modulation have been applied to bandpass signal frequency ranges whose frequency content lie in a narrowband [1, p. 282]. The implication of this is that Σ–Δ modulation can now be employed to perform Analog-to-Digital (A/D) conversion for higher frequencies with restricted bandwidth in comparison to the lowpass case. Bandpass Σ–Δ modulators are designed such that most of the quantisation noise is shaped to either side away from the signal band of interest. The original signal is retained virtually unaffected with very little noise in the desired frequency range. A typical application for bandpass A/D conversion is in digital radio systems where the IF signal of a superhetrodyne radio receiver can be directly converted to a digital representation [1, p. 282]. Other applications include AM digital radios and receivers for digital cellular mobile radios [2, p. 353]. An extension of Shannon's Sampling Theorem to bandpass signals stipulates that the sampling frequency has to be only twice the bandwidth of the signal implying that much higher OverSampling Ratios (OSR) can be attained for relatively modest sampling frequencies [2, p. 354]. The example under consideration in this paper elaborates on sinusoidal inputs centred at 2.5 MHz sampled at 10 MHz for three different OSRs.

In order to obtain acceptable in-band noise performance for medium to high resolution applications, either higher-order single-loop structures or increased OSRs have to be employed. Both options have their drawbacks [3]. A well known approach with guaranteed stability is the oversampled bandpass MultistAge noise SHaping (MASH) Σ–Δ modulator [3]. Two novel effective-fourth-order resonator based MASH bandpass Σ–Δ modulators are introduced, examined by exhaustive simulations at the behavioural level. Their results in both time and frequency domains are compared to identify the merits and drawbacks of each structure. Both effective-fourth-order MASH structures consist of a cascade connection of simple to implement lossless resonator based bandpass structures [4].

The organisation of this paper is as follows. An overall explanation together with an exposition of the internal structure of each of the two structures is given in Section 2. Section 3 illustrates and briefly explains the structure and function of the standard second-order resonators and notch filters. Section 4 presents a method for assessing the performance of these structures based on theoretical calculations and then compares these mathematical results with the detailed simulations conducted at the behavioural level. Section 5 provides an explicit comparison of both structures based on both theoretical and empirical results.

2. THE DIFFERENT MODULATOR ARCHITECTURES

2.1 Quadruple Effective-First-Order (1-1-1-1) Cascade

The first structure considered is known as an effective-fourth-order MASH bandpass Σ–Δ modulator which is a cascade of four effective-first-order Σ–Δ modulators. The quantisation error of the first stage is fed to the input of the second stage. Similarly; the quantisation error of the second stage is fed to the input of the third stage and likewise for the fourth stage. The output of the modulator is the sum of the first stage, the second stage notch filtered once, the third stage doubly notch filtered and the fourth stage notch filtered thrice. The output signal in the time domain from the 1-1-1-1 shows that the modulator produces values of odd numbers in the range of $\pm$ 15. The output signal of the first stage which has values $\pm$ 1 after the one notch filter becomes a signal which consists of samples having one of three amplitudes 0 and $\pm$ 2. Similarly; a double notch filter yields a signal having values of 0, $\pm$ 2 and $\pm$ 4 and the third notch filter produces values of $0, \pm 2, \pm 4$ and ± 8. All the combinations from each of the four stages are added to produce the final output signal having one of the following values $\pm 1, \pm 3, \pm 5, \pm 7, \pm 9, \pm 11, \pm 13$ and $\pm$ 15. The cumulative effect of the multi-bit output was verified by taking a histogram of the output signal for 33000 samples for different input amplitudes and oversampling ratios.

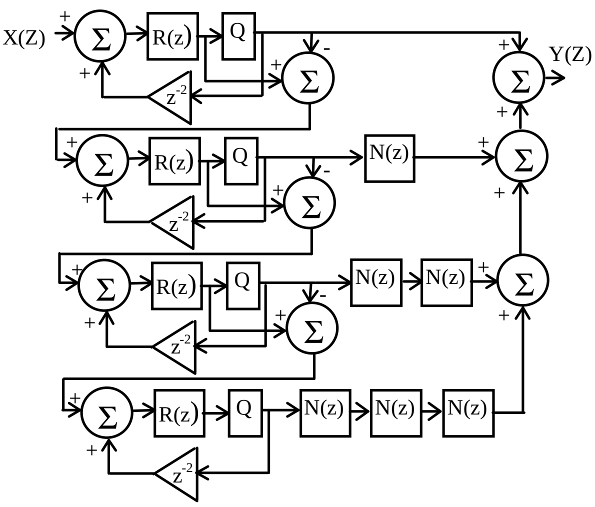

Figure 1: Block diagram of the quadruple effective-first-order cascade.

Frequency domain simulations employing a non-linear single-bit quantiser demonstrated that most of the noise was shaped away from the desired band of interest. Dither in the form of additive white Gaussian noise scaled by 0.01 is added to each stage just before the quantiser. A simplified overall output expression in the z-domain is obtained by modelling the non-linear quantiser with additive white noise. This is given by

$$Y_1(z) = X(z) + (1 + z^{-2})^4 Q_{14}(z) \qquad (1)$$

where *X(z)* is the input, $Q_{14}(z)$ is the quantisation noise of the fourth stage, *R(z)* is the second-order resonator and *N(z)* is the second-order notch filter.

2.2 Effective-Second-Order Effective-Second-Order (2-2) Cascade

The second architecture considered is a cascade combination of two effective-second-order modulators yielding an overall effective-fourth-order MASH bandpass Σ–Δ modulator. The first stage consists of two second-order resonator sections and a one bit quantiser in the feedforward path. The quantisation noise of the first stage is fed to the input of the second stage. The output is the sum of the double delayed version of the first stage and the double notch-filtered version of the second stage. The output signal in the time domain from the 2-2 structure and its corresponding histogram for 33000 samples shows that the 2-2 modulator produces values of odd numbers in the range of $\pm$ 5. The first stage has output values of $\pm$ 1. The second stage which incorporates a double notch filter produces output values of $0, \pm 2$ and ± 4. Output combinations from both stages are added to produce the final output signal having one of the following values $\pm 1, \pm 3$ and ± 5. The reduced usage of notch filters results in fewer multi-bit output combinations. This was verified by taking a histogram of the output signal for 33000 samples for a variety of input amplitudes and oversampling ratios. Modelling the non-linear quantiser as an additive white noise source having identical features to that discussed in section 2.1 yields an overall output in the z-domain which is given by

$$Y_2(z) = z^{-4} X(z) + (1 + z^{-2})^4 Q_{22}(z) \qquad (2)$$

where *X(z)* is the input, $Q_{22}(z)$ is the quantisation noise of the second stage, R(z) is the second-order resonator and $N^2(z)$ is two second notch filters in cascade.

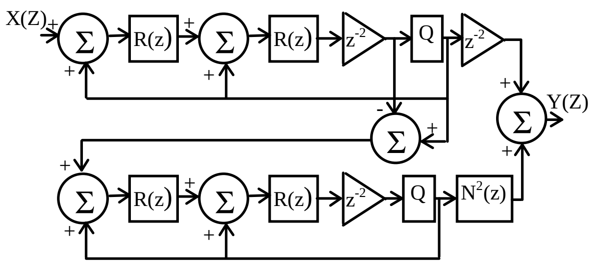

Figure 2: Block diagram of the effective-second-order effective-second-order cascade.

3. RESONATOR & NOTCH FILTER CONFIGURATIONS

3.1 The Second-Order Resonator

Each of the two effective-fourth-order narrowband MASH bandpass Σ–Δ modulators employed the simple second-order resonators with unity feedback [4]. The z-domain transfer functions of the resonators *R (z)* is given by

$$R(z) = z^2/(z^2+1) \tag{3}$$

where the zeros are stationed at the origin (z = 0) and the two complex conjugate poles are placed at the half Nyquist frequency ($z = \pm j$) thus achieving resonance at one quarter of the sampling frequency.

3.2 The Second-Order Notch Filter

This is a simple second-order notch filter having two complex conjugate zeros at ($z = \pm j$) and two poles stationed at the *z*-plane origin (*z* = *0*) where the transfer function in the z-domain *N(z)* is given by

$$N(z) = (z^2+1)/z^2 \tag{4}$$

4. IN-BAND SIGNAL-TO-NOISE RATIO (SNR)

4.1 Theoretical Calculations

A major measurement parameter for assessing the performance of any Σ–Δ modulator is its in-band signal-to-noise ratio (SNR) [5, p. 150]. A general-case mathematical expression based on the additive noise model was developed by the authors from first principles for any narrowband bandpass Σ–Δ modulator and is shown below

$$S_B = S_Q \, g \, / \, f_S \int_{f_O - f_B/2}^{f_O + f_B/2} \left(H_1(f)\right)^{2n} df \tag{5}$$

where $H_1(f)$ is the noise shaping transfer function of a single stage and is given by

$$H_1(f) = 2\cos 2\pi \frac{f}{f_S} \tag{6}$$

where S_B is the total in-band noise power of the modulator, f_S is the sampling frequency, f_O is the resonant centre frequency, f_B is the bandwidth, S_Q is the quantiser error, *n* is the modulator order and *g* is an architecture dependent scaling coefficient set to 1 in the results presented in this paper.

The theoretical in-band SNRs were evaluated incorporating (5) and (6) for three different OSRs for each of the two architectures. These OSRs were 128, 64 and 32 giving theoretical in-band SNRs of 164 dB, 137 dB and 110 dB respectively for both structures for a sinusoidal input having full scale amplitude, f_O of 2.5 MHz and f_S of 10 MHz.

4.2 Behavioural Level Simulations

Various simulations were conducted at the behavioural level for both architectures for sinusoidal inputs of different amplitudes for three OSRs to assess their performance and make comparisons between the theoretical and practical simulation results.

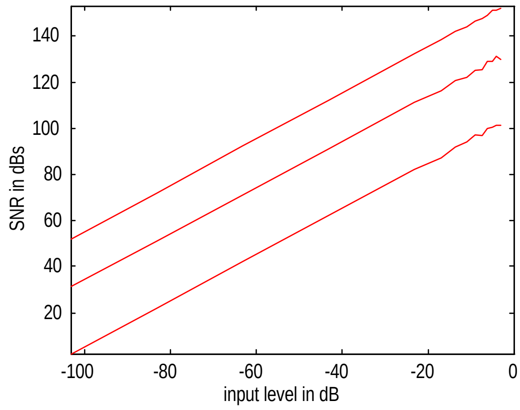

Figure 3: SNR plots to compare different OSRs for (1-1-1-1) cascade structure.

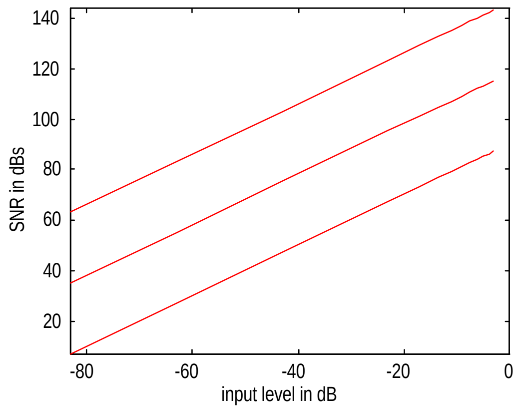

Figure 4: SNR plots to compare different OSRs for (2-2) cascade structure.

The first set of results shown in Figure 3 illustrate the relationships for the in-band SNRs for three OSRs of 128, 64 and 32 for the 1-1-1-1 cascade. Figure 4 provides a similar graphical representation for the various OSRs of the 2-2 cascade. The main conclusions drawn from these results are that the SNR curves for the 1-1-1-1 cascade MASH structures are significantly better by as many as two bits of resolution in comparison to those obtained from the 2-2 cascade for all three OSRs.

The next category of simulations illustrate the relationship between the calculated theoretical in-band SNRs for the two different architectures for OSRs of 128 and 64 against the input amplitude respectively. Thus, Figure 5 illustrates the three SNR curves, the first representing the theoretical in-band SNR based on the derived formula and the remaining two represent the SNR curves based on the two architectures for an OSR of 128. Figure 6 shows a similar comparison for an OSR of 64.

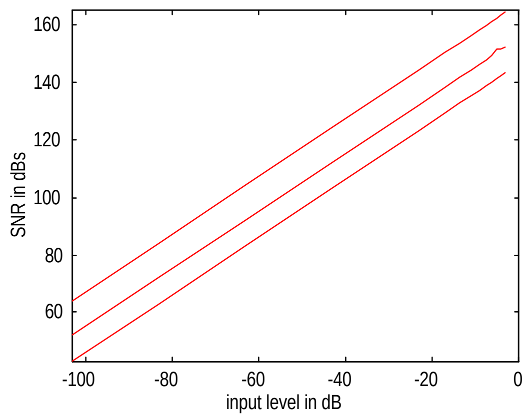

Figure 5: A comparison of SNR plots between theoretical, (1-1-1-1) and (2-2) cascade structures for an OSR = 128.

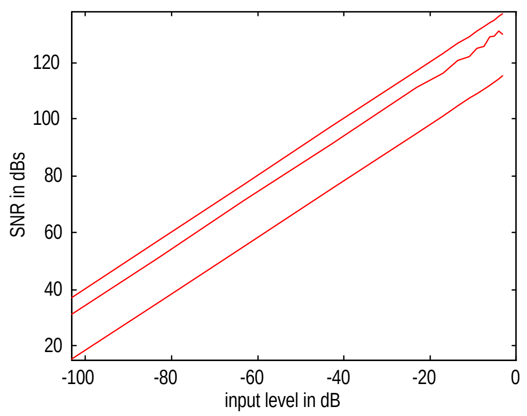

Figure 6: A comparison of SNR plots between theoretical, (1-1-1-1) and (2-2) cascade structures for an OSR = 64.

5. CONCLUSIONS

As can be seen from the reported results, the 1-1-1-1 cascade structure produces improved in-band SNR for all the three OSRs compared with its contemporary counterpart the 2-2 cascade structure. This superior performance can be attributed to the cumulative effect of the multi-bit signals present in the structure as well as the multistage notch filters (6 of them) compared with the 2-2 cascade that only has two notch filters. The main advantage of the 2-2 structure, however, is that the quantisation noise of the first stage output produces effective-second-order noise-shaping which is much smaller in magnitude and therefore rendering effects of component mismatches between the first and second stages are less significant [3, p. 147]. The second advantage is that fewer notch filters are needed to produce the same final transfer function, thus making it a cheaper structure to implement. The SNR results from simulations were found to be 7dB lower with their equivalent theoretical values for the 1-1-1-1 cascade structure for an OSR of 64. Similarly; these simulated SNRs were found to be 18dB lower compared with their corresponding theoretical values for the 2-2 cascade for the same OSR. It can be concluded that the 1-1-1-1 cascade structure has significantly better in-band SNR performance as well as conforming more closely with theory compared with the 2-2 cascade for different OSRs at the expense of increased hardware complexity and higher sensitivity to component mismatches.

REFERENCES

[1] Jantzi, S. A., M. Snelgrove and P.F. Ferguson, “A Fourth-Order Bandpass Sigma-Delta Modulator”, *IEEE Journal of Solid-State Circuits*, vol. 28, no. 3, March 1993.

[2] Gourgue, F., M. Bellanger, S.Azrouf and V. Bruneau, “A Bandpass Subsampled Delta-Sigma Modulator for Narrowband Cellular Mobile Communications”, *IEEE International Symposium on Circuits and Systems*, vol. 5, 1994.

[3] Ribner, D.B., “A Comparison of Modulator Networks for High-Order Oversampled Sigma-Delta Analog-to-Digital Converters”, *IEEE Transactions on Circuits and Systems*, vol. 38, no. 2, pp. 145-159, February 1991.

[4] Ribner, D.B., “Multistage Bandpass Delta Sigma Modulators”, *IEEE Transactions on Circuits and Systems-II*, Analog and Digital Signal Processing, vol. 41, no. 6, pp. 402-405, June 1994.

[5] Al-Janabi, M., I. Kale and R.C.S. Morling, “Measurement and characterisation of MASH bandpass sigma-delta modulators for direct IF analog-to-digital conversion”, *Proc. IMEKO Workshop “ADC Modelling”*, pp. 147-152, Slovak Republic, 7-9 May 1996.